

Electrochemical Discharge Drilling of Inclined Micro Holes with Step Feeding Method

Hang Yusen, Xu Zhengyang*, Wang Feng, Zhang Chenxiang

National Key Laboratory of Science and Technology on Helicopter Transmission, Nanjing University of Aeronautics and Astronautics, Nanjing 210016, China

*E-mail: xuzhy@nuaa.edu.cn

Received: 25 September 2019 / *Accepted:* 6 December 2019 / *Published:* 10 February 2020

Film cooling holes are distributed mainly on the surface of turbine blades, with center lines at angles to the tangential direction. These “inclined micro holes” (IMHs) are difficult to machine because of their extremely small diameters, the challenge of cutting metal materials, and the high requirements for machining quality/efficiency. To achieve machining of IMHs, we employed an electrochemical discharge drilling method. The recast layer, however, remained at the outlet of IMHs due to the turbulent flow field and short electrolysis time at the outlet. To improve further the processing quality of IMHs, step feeding of electrode was used to prolong the electrolysis time (i.e., the tool electrode was stopped for a short time after penetrating the workpiece). Changing the feed rate and increasing the pause time of electrode (PToE) led to continuation of electrolysis after penetration of the electrode out of the IMH. Electrochemical dissolution around the IMH was sufficient to improve removal of the recast layer. Therefore, IMHs without a recast layer were obtained. Experiments with different PToE were carried out, and analyses of voltage waveforms, current waveforms, average diameter, IMH morphology, and elimination of the recast layer on IMH walls undertaken. Results showed that step feeding method could corrode the residual recast layer at the outlet of IMHs.

Keywords: Film cooling hole; Electrochemical machining (ECM); Electrical discharge machining (EDM); Electrochemical discharge drilling (ECDD); Inclined micro hole (IMH); Step feeding; Pause time of electrode (PToE); Recast layer

1. INTRODUCTION

The core components of an aerospace engine are turbine blades. The latter are “guide” blades and “working” blades, and are required to work at a temperature above the melting point of the material of which the engine blade is made [1, 2]. Therefore, film cooling has become a widely applied method to prevent the blade from being damaged by high temperature [3]. The most important components of the film-cooling method are film cooling holes. These are located extensively on the surface of blades

and vanes [4] and with center lines at angles to the tangential direction. The spatial positions of these “inclined micro holes” (IMHs) are extremely complicated, and are characterized by small diameters and large numbers [5]. Continuous optimization of a turbine engine also imposes strict requirements on the quality of the film cooling holes. Processing of film cooling holes must ensure an absence of heat-affected zones, micro cracks and recast layers [6]. Thus, IMH manufacture has become a key issue for the improvement of aeroengine quality.

McGeough et al. [7] undertook an experimental study on improving surface quality by hybrid processing based on electrical discharge machining (EDM) and electrochemical machining (ECM). Hung et al. [8] combined EDM with electrochemical polishing, using electrochemical dissolution to polish IMH walls after EDM [9, 10]. This method can eliminate the burrs and recast layer, and reduce the tapering and roughness, of the IMH wall. Kurita and Hattori [11] investigated the method of machining smooth surfaces by electrolytic grinding after EDM. Using deionized water, Chung et al. [12] investigated the IMH surface achieved by micro-EDM based on ECM [13] corrosion, and the effects of processing factors on surface roughness. Nguyen et al. [14] proposed a processing method in which micro-ECM is carried out after micro-EDM during machining. This method can improve the surface finish and processing precision. These processing methods can further improve the surface quality of IMHs through the cooperation of two processing forms, one before and the other after. Plaza et al. [15] discovered that use of a helical electrode in micro-EDM drilling could shorten the processing time, but that wearing down of the electrode occurred and the processing cost is increased. Zhang et al. [16] postulated an electrochemical discharge drilling (ECDD) method combining EDM and ECM in which the two processing modes elicited their effects simultaneously. This processing method features the high-speed perforation of EDM, the advantages of ECM (no residual processing stress, surface micro-cracks or electrode losses [17]) and the surface obtained by composite processing is also smoother [18, 19]. In addition, this composite processing method is also effective for the processing of non-metallic materials. Garg et al. [20] used an electrochemical discharge machining method to realize the micro-drilling of carbon fiber-reinforced polymer composites.

We undertook ECDD experiments of IMHs to explore the effect of composite processing on the structure of IMHs. To further remove the residual recast layer on IMHs, an experiment was carried out to optimize the pause time of electrode (PToE) by stopping the tool electrode for a short time after its penetration into the workpiece. Experiments revealed that the residual recast layer could be removed completely. Finally, IMHs without recast layers were obtained with the optimum PToE.

2. EXPERIMENTAL DETAILS

2.1. Method of step feeding

Figure 1 shows the penetration stage and pause stage of IMHs. The electrolyte flows through the inner hole of the tube electrode, and flows out from the exit of the hole during the penetration stage of ECDD, and reverse flushing develops rapidly in the side gap. Processing of spark discharge and electrolytic processing occur simultaneously. The workpiece anode is penetrated fully, but the electrolytic effect occurs only in the lateral gap to corrode the residual recast layer further (Fig. 1). This

is because the lateral gap increases more than the spark gap, resulting in the electrolytic effect occurring only in the gap.

Due to the existence of a certain inclination angle, an uneven flow field occurs readily in the machining of IMHs. The tube electrode withstands the non-metallic contrast layer after it penetrates the workpiece, causing a decrease of the reverse liquid and turbulence of the flow field. These actions can result in the remains of the recast layer on the exit of the IMH. To penetrate the IMH completely, the tube electrode has a greater depth of feeding. Bending and radial shaking of the tube electrode are extremely likely to occur in the presence of the contrast layer. These actions result in an unevenness of the flow field and short circuit discharge, which affects the processing stability and elimination of the recast layer of the IMH.

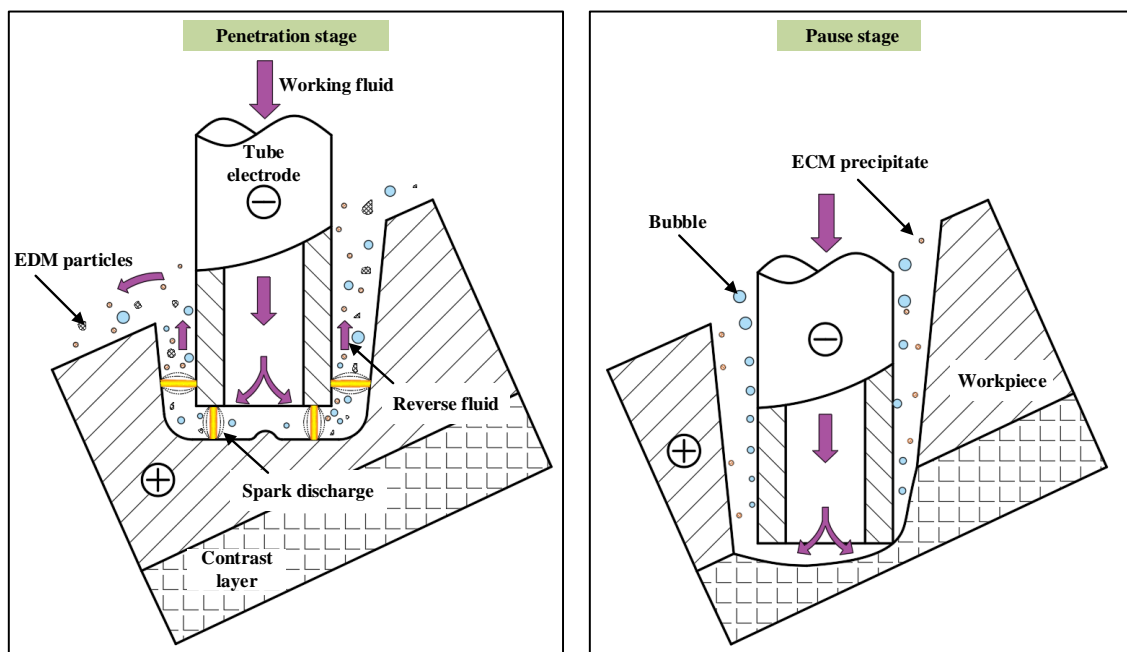


Figure 1. Step processing stages of IMHs (schematic)

Step feeding of electrode can be used to solve the problem of incomplete elimination of the recast layer raised by flow-field disturbance during processing. In this method, the tube electrode is stopped for a short time when it withstands the non-metallic contrast layer (Fig. 1). The reverse flushing channel in the lateral gap can be formed again with flushing and rotation of the electrolyte in sufficient time. The recast layer on exit of the IMH can be corroded with sufficient time. This method prolongs the machining time of ECM, thereby realizing further removal of the recast layer and achieving processing of IMHs without recast layers.

2.2. Machine tool

Experimental research was undertaken on an electrochemical discharge machine tool. Processing of IMHs was realized by rotation of the principal axis (Figs. 2 and 3). The horizontal direction was the benchmark. The inclination angle was the angle between the level of the machine tool and the

benchmark. We used a six-axis computerized numerical control machine tool that could process film cooling holes with complex angles.

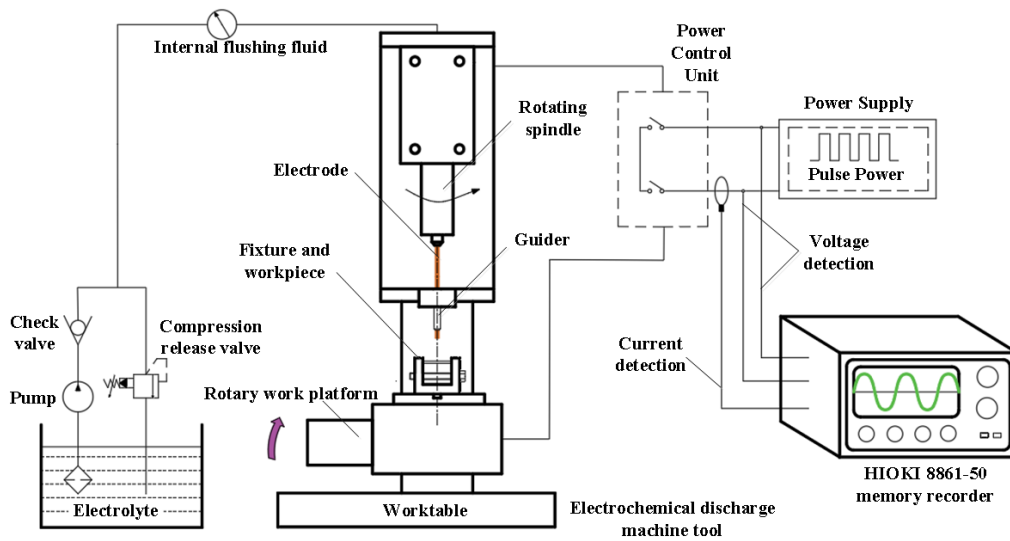


Figure 2. Electrochemical discharge machining system

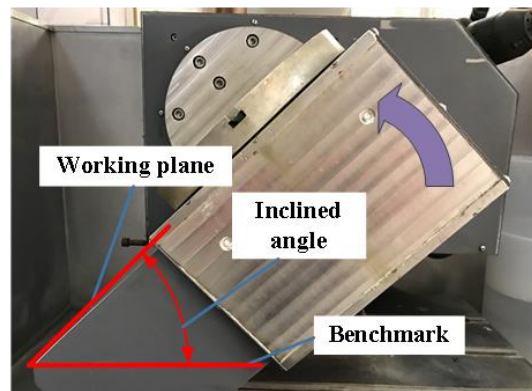


Figure 3. Photograph of the machine tool of inclined hole

The ECDD system is displayed as Fig. 3. The drilling system comprised a: power supply unit; circulation system for working fluid; three-dimensional motion platform; detection unit of voltage; recorder of current waveforms. In the working-fluid circulation system, the electrolyte was ejected from the inner hole of the high-speed rotating tube electrode, thereby forming a processing channel between the electrolyte and workpiece. The tube electrode was clamped in the rotating spindle. Voltage waveforms and current waveforms were documented by a memory recorder (8861-50; Hioki, Ueda, Japan) during IMH machining.

2.3. Experimental method

To simulate the true processing of the film cooling holes of the turbine blade, we conducted

experiments of electrochemical discharge machining of IMHs at 30°. To improve the surface quality of the IMHs and removal of the recast layer, different PToE at the end of the processing was used. Table 1 lists the main experimental parameters of IMH processing.

Table 1. Main experimental parameters

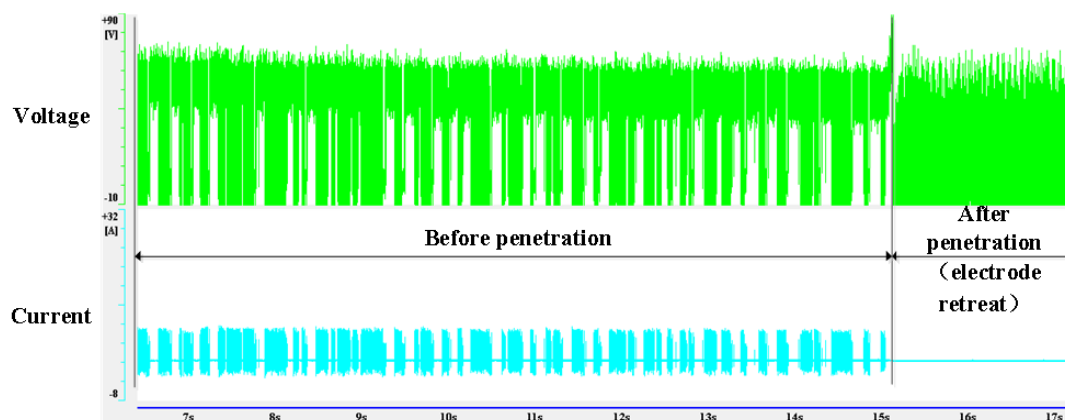
Parameter	Value
Voltage amplitude	80V
Peak current	8 A
Pulse interval	20 μ s
Pulse duration	12 μ s
Flushing pressure	6.5Mpa
Working liquid	3g/L NaNO ₃ solution
Conductivity of working liquid	4mS/cm
External diameter of electrode	Φ 300 μ m
Length of electrode	200mm
Rotational speed of electrode	100rpm
Material of workpiece	Nickel base superalloy
Thickness of working piece	2mm
Inclined angle	30°
Pause time of electrode	0,2,4,6,8s

During processing, the memory recorder (8861-50; Hioki) was used to record the voltage waveforms and current waveforms, and the processing time of the IMH was recorded simultaneously. After machining, the average diameter was measured by a plug gauge and microscope (DVM5000; Leica, Wetzlar, Germany). The morphology of the hole inlet and hole outlet was observed by a scanning electron microscope (S-3400N; Hitachi, Tokyo, Japan). Finally, metallographic examination of the IMHs was carried out. Also, the residual recast layer was observed by means of a microscope (DVM5000; Leica).

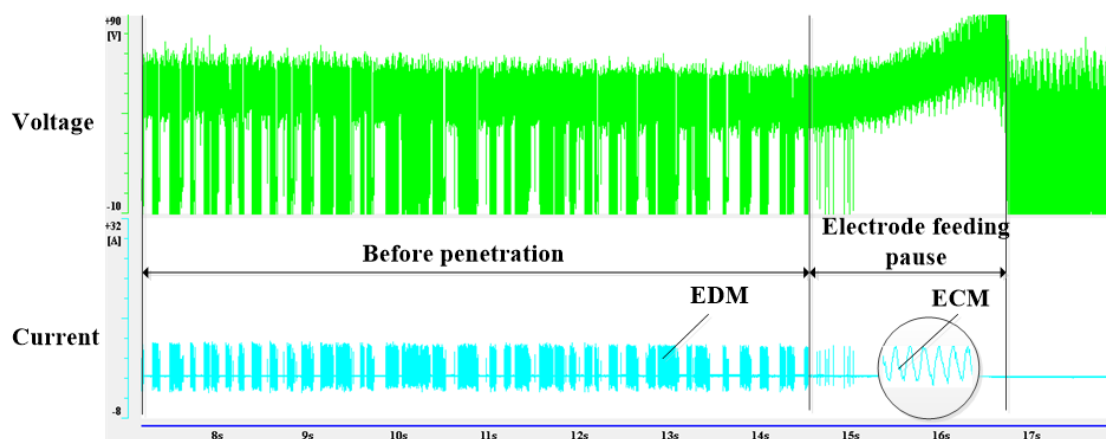
3. EXPERIMENTAL RESULTS AND DISCUSSION

3.1. Waveform analyses

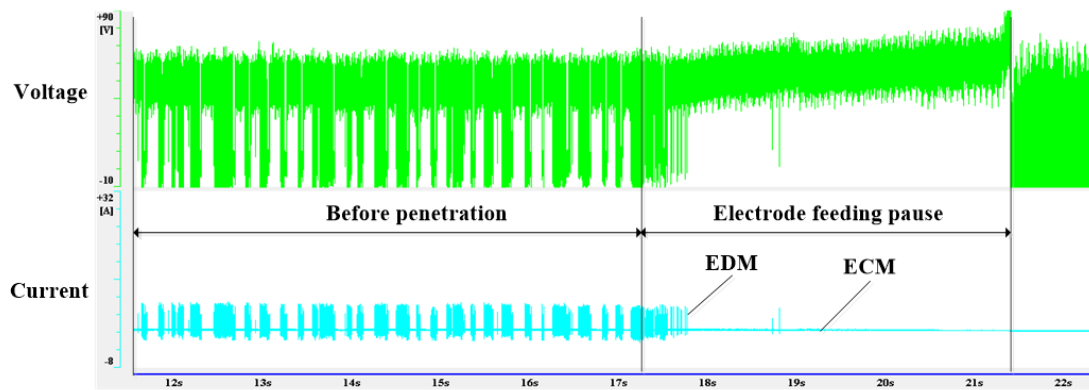
Figure 4 displays the voltage waveforms and current waveforms during the processing with different PToE. Figure 4(a) exhibits the waveform with a PToE of 0 s. When the IMH had been penetrated completely, the tube electrode started to retreat. Figure 4(b), (c), (d) and (e) display the waveforms with a PToE of 2, 4, 6 and 8 s, respectively. Figure 4(b), (c), (d) and (e) show a slight effect of EDM at the beginning of the pause stage, and the absence of the effect of ECM during the posterior segment of this pause. This effect was due to the inclined contrast layer against one side of the tube electrode after the workpiece had been penetrated. This led to a decrease of the reverse liquid as well as bending and radial shaking of the electrode at the beginning of the pause of electrode feeding. With flushing and rotation of the electrolyte, the non-metallic contrast layer in contact with the electrode could be washed out and a dent was formed. Therefore, the electrode could recover stable rotation and the working fluid in the lateral gap could circulate smoothly.



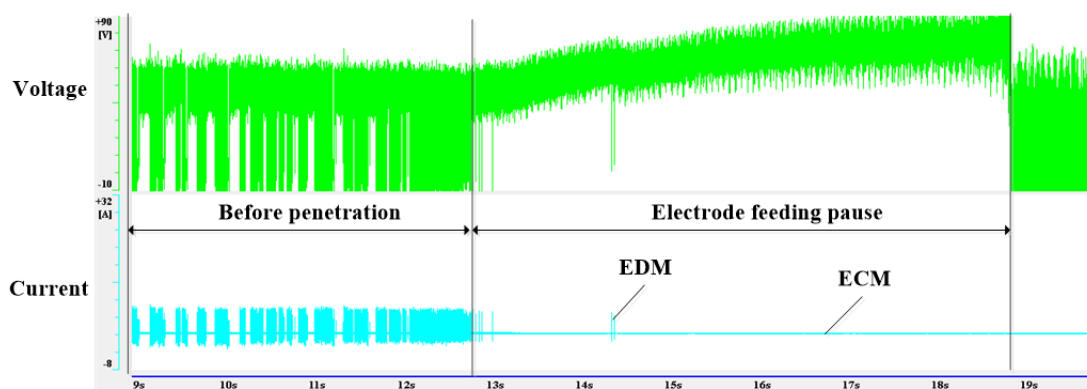
Voltage waveforms and current waveforms with a PToE of 0 s



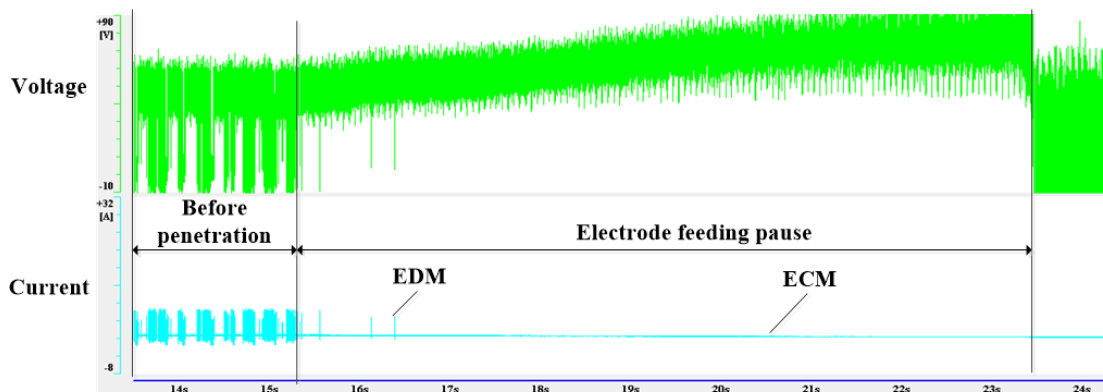
Voltage waveforms and current waveforms with a PToE of 2 s



Voltage waveforms and current waveforms with a PToE of 4 s



Voltage waveforms and current waveforms with a PToE of 6 s



Voltage waveforms and current waveforms with a PToE of 8 s

Figure 4. Voltage waveforms and current waveforms during processing of IMHs with different PToE

A comparison of Fig. 4(a) and (b) reveals that the pause of electrode prolonged the electrolysis time. When the inclined hole is penetrated, the gap between the hole wall and the tube electrode is larger than the spark discharge gap, so that only the electrolytic effect is left in the pause phase. This result is in agreement with the reports by Zhang [21] and Sumit [22]. Zhang reported that when the lateral gap exceeds the critical discharge gap, the removal of the work-piece material is mainly by electrochemical

corrosion [21]. Sumit reported that sparks are generated only from the tip of the tool and so the diametrical overcut is reduced [22]. Figure 4(b)–(e) indicate that, with an increasing PToE, the longer the ECM effect, the better was the effect of removal of the recast layer.

3.2. Analyses of IMH diameters

A longer time of ECM can also result in an increase of the average diameter of an IMH. The inlet diameter and outlet diameter of IMHs at different PToE, with a tube electrode of diameter 300 μm , are displayed in Fig. 5. The inlet diameter and outlet diameter presented an increasing trend with increasing PToE. Also, enlargement of the outlet diameter was greater than that of the inlet diameter. This effect was because the lateral gap in the outlet was smaller than that in the inlet during electrode penetration with ECM. The electrochemical efficiency of the outlet was higher, and the reaming effect of the outlet was more obvious. The reaming efficiency was worst for a PToE of 2 s, which was due to the: (i) slight effect of EDM at the beginning of the pause stage; (ii) short electrolysis time (Fig. 4(b)).

Figure 6 displays the average diameter (i.e., the average value of the outlet diameter and average value of the inlet diameter) and the taper angle at different PToE. The average diameter showed a large range of increase: from 471.380 μm to 592.267 μm . This result is in agreement with that from a report by Fan et al. They reported that a large pulse on-time caused a large diameter of the IMH [23]. The pulse on-time represents the processing time during the pulse period: the larger the pulse on-time, the longer is the electrolysis time. Meanwhile, with an increase of PToE, the taper angle decreased almost linearly, the taper is reduced by 72.5 percent in total. As explained by Ali et al., the smaller the feed rate, the longer is the electrolytic processing time and the smaller is the taper of small holes [24]. That is, step feeding of electrode prolonged the electrolytic processing time effectively, and could reduce the taper of IMHs.

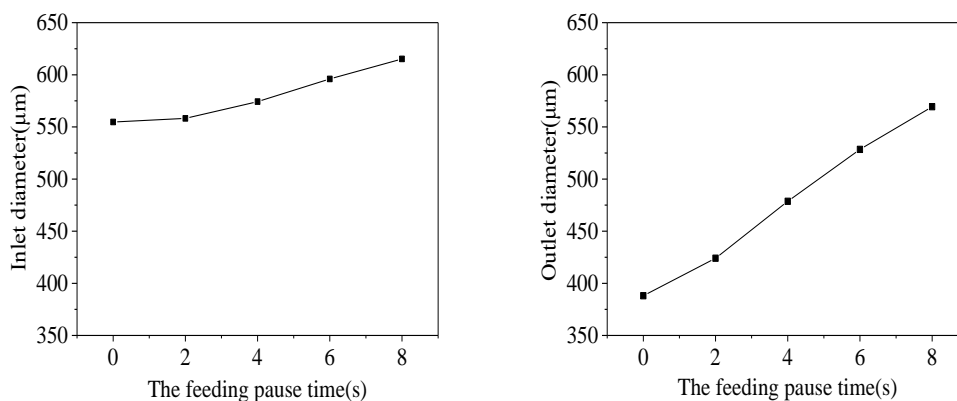


Figure 5. Inlet diameter and outlet diameter at different PToE

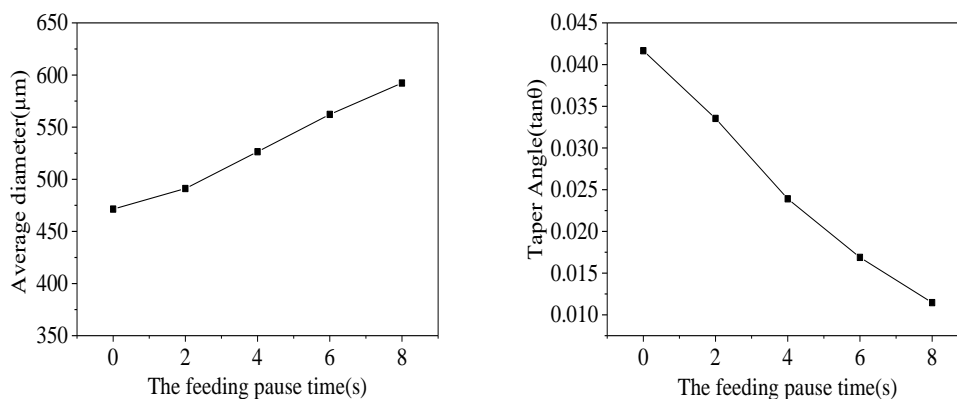


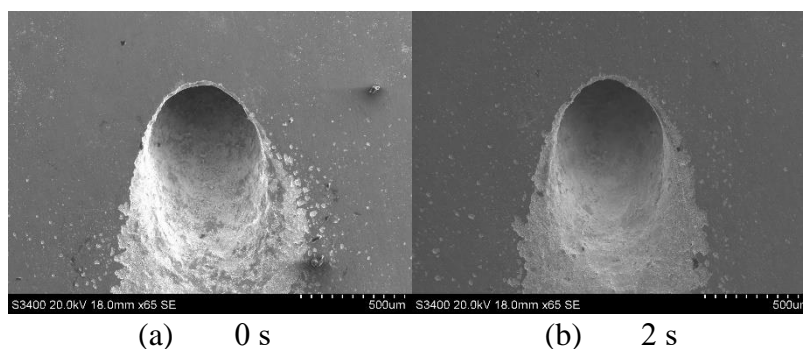
Figure 6. Average diameter and taper angle at different PToE

3.3. Morphology

IMH morphology after processing was analyzed by scanning electron microscopy. Figures 7 and 8 show the inlet morphology and outlet morphology of IMHs with PToE of 0, 2, 4, 6 and 8 s, respectively. The shape of the inlet and outlet was oval, and obvious spurious corrosion on the inlet of IMHs was visible. One reason for this phenomenon could be that reverse flushing accumulated on the inlet surface and then the electrolysis time became longer at the inlet. Hence, ECD could be used to process well-shaped IMHs.

The morphology of the IMH inlet with different PToE is displayed in Fig. 7. The comparison between Fig. 7(a), (b) and (c)–(e) show that when the PToE was increased, the IMH wall became smoother and the shape more rounded. Hence, step feeding of the electrode could prolong electrolysis. Figure 8 shows that the IMH outlet became a more rounded ellipse as the PToE increased. In addition, the diameter of the IMH outlet continued to increase due to the longer processing time. In summary, when the PToE was >2 s, a better appearance of the IMH could be obtained.

The morphology of the inclined hole inlet with different PToE is displayed in Fig. 7. The comparison between Fig. 7(a), Fig. 7(b) and Fig. 7(c)–(e) shows that when the PToE is increased, the hole wall becomes smoother and the shape more rounded. This means that the method of step feeding can prolong the electrolysis. The PToE has more impact on the inclined hole outlet. Figure 8 exhibits that the morphology of the hole outlet is a more rounded ellipse as the PToE increases. Additionally, the diameter of the inclined hole outlet keeps growing due to the longer processing time. In summary, when the PToE is longer than 4s, a better appearance of the inclined hole can be obtained.



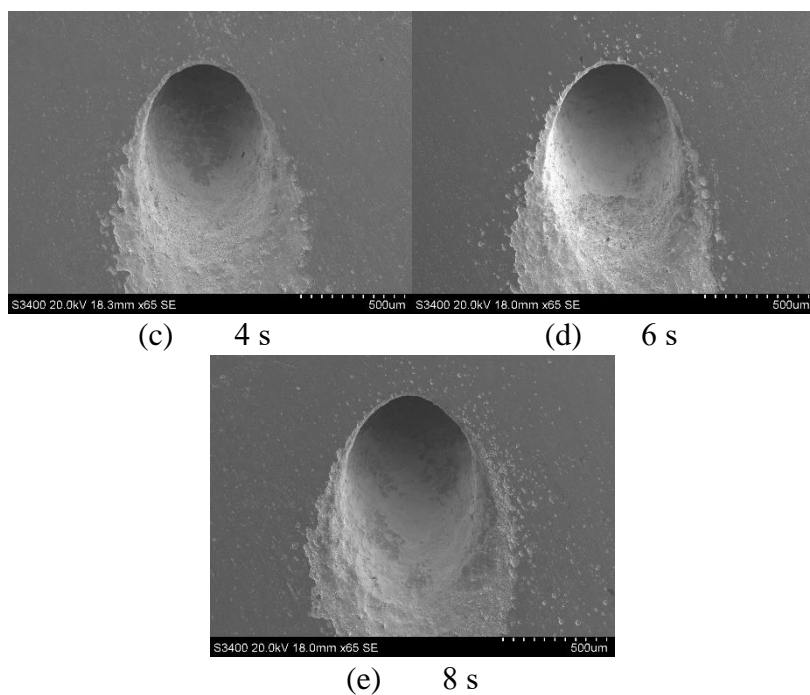


Figure 7. IMH morphology with different PToE

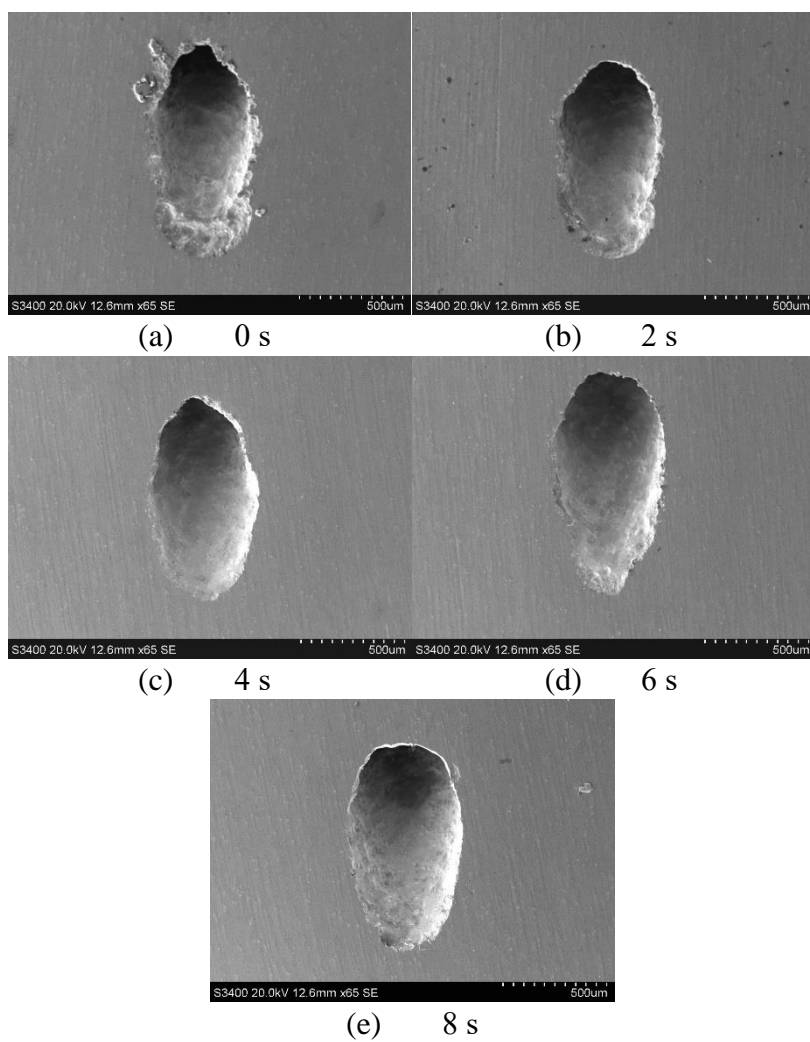


Figure 8. Morphology of the IMH outlet with different PToE

Figure 9 displays the cross-section morphology of IMHs with different PToE. The flaw of the IMH wall decreased with increasing of IMH parameters at different PToE. In particular, Fig. 9(a) and (b) show the worst morphology of IMHs. The partial enlargement map shows obvious corrosion pits on the IMH wall. When the PToE reached 4s, the defects on the IMH wall were eliminated under electrolytic action. This explains that a long electrolysis time could obtain a better surface. This is consistent with the conclusion of Zeng et al. They demonstrated that the surface quality can be improved as the feed rate decreases, that is, a longer electrolysis time [25]. Therefore, 4, 6 and 8 s were suitable parameters for the PToE. Meanwhile, with the increasing of PToE, the decrease of taper is shown directly in Fig. 9(a)–(e).

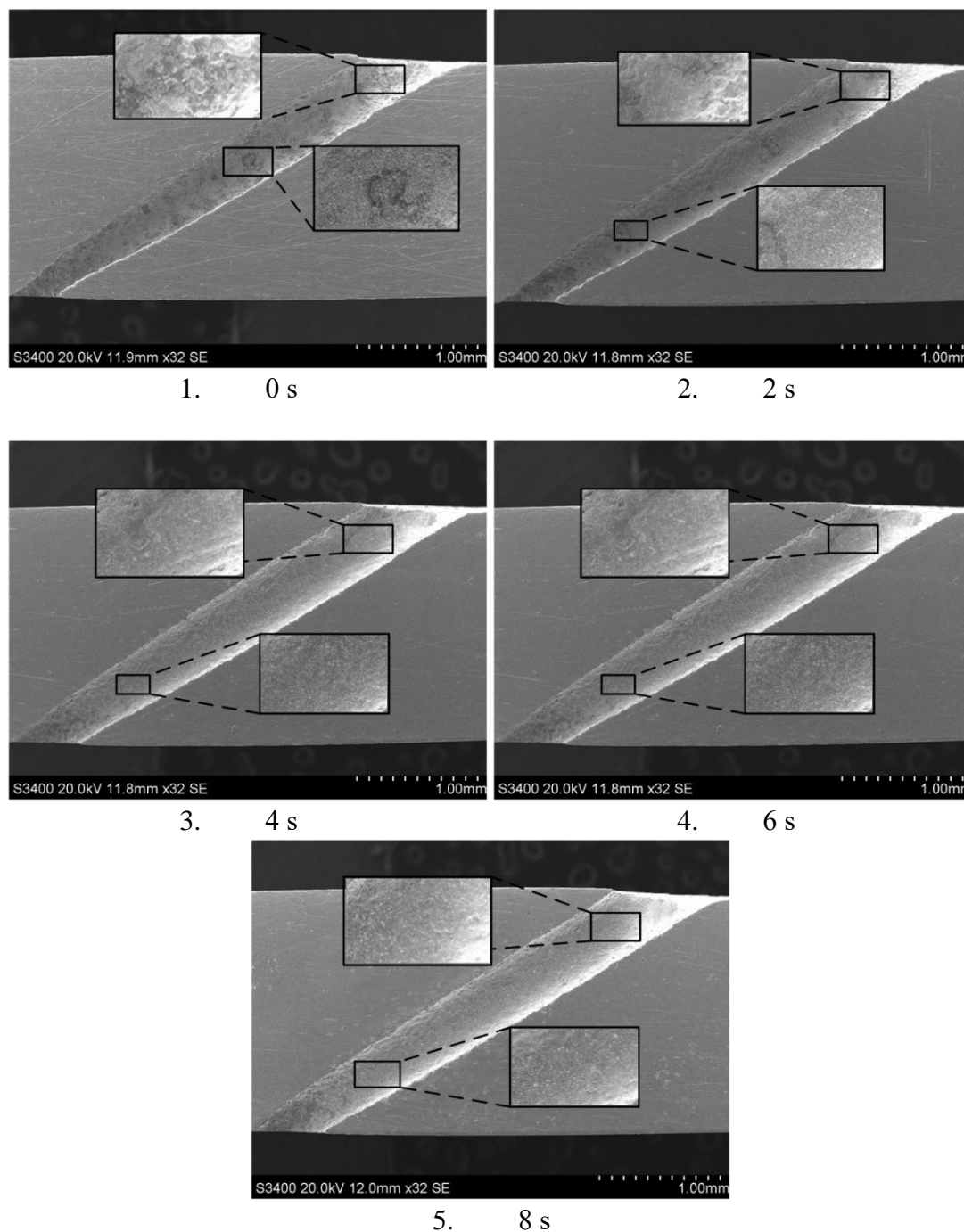


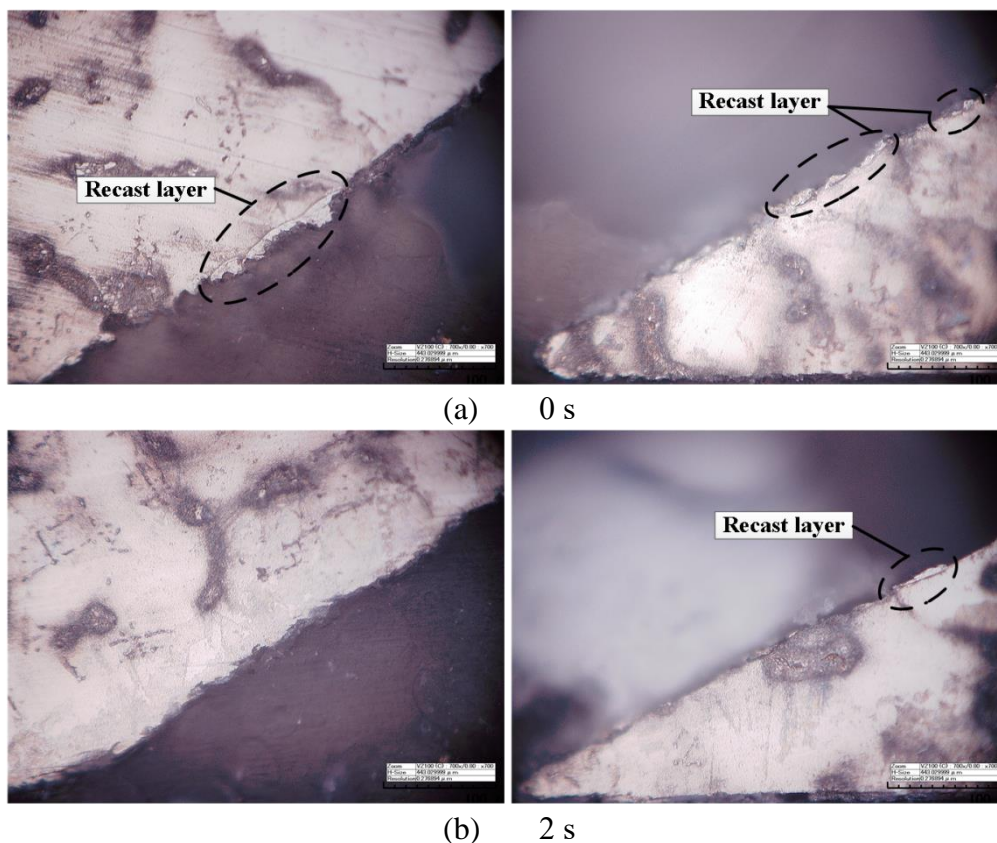
Figure 9. Cross-section morphology of the IMHs with different PToE

3.4. Analyses of the recast layer

Figure 10 shows the residual recast layer at the IMH outlet with different PToE. Figure 10(a) displays the residual condition of the recast layer during no pause of electrode feeding. This layer was concentrated at the IMH outlet, whereas the recast layers at the inlet and in the middle of IMHs were removed completely. This happened because electrolysis at the IMH inlet was relatively longer than that at the IMH outlet. Therefore, the recast layer at the upper part and middle part of IMHs could be dissolved completely with sufficient time of electrolysis, and a thin recast layer remained at the outlet because the electrolysis time of this part was relatively short.

Part of the recast layer at the IMH outlet remained when the PToE was set to 2 s (Fig. 10(b)). When the PToE was increased to >2 s, the residual recast layer on the IMH wall was removed completely (Fig. 10(c)–(e)). The results showed that step feeding of electrode could increase the electrolysis time and enhance the effect of electrochemical dissolution at IMH outlet processed by ECDD.

The IMH wall became smoother as the PToE increased (Fig. 10(a)–(e)). At 0 s and 2 s, the IMH wall presented an irregular straight-line shape, or even a slightly curved one. When the PToE reached 4 s, the curve disappeared, but the straightness of the IMH wall remained poor. When the PToE reached 6 and 8 s, the quality of the IMH wall had improved considerably. Hence, the pause of electrode improved the quality of the IMH wall, and eliminated the recast layer completely. This result is in accordance with data from Zeng [26] and Chung [27]. Zeng stated that the surface quality of the workpiece was enhanced and the recast layer was removed by combination with ECM [26]. Chung successfully obtained a smooth surface with ECM in deionised water [27]. Electrolysis was effective for removal of the recast layer. The longer the electrolysis time, the more thorough was the removal.



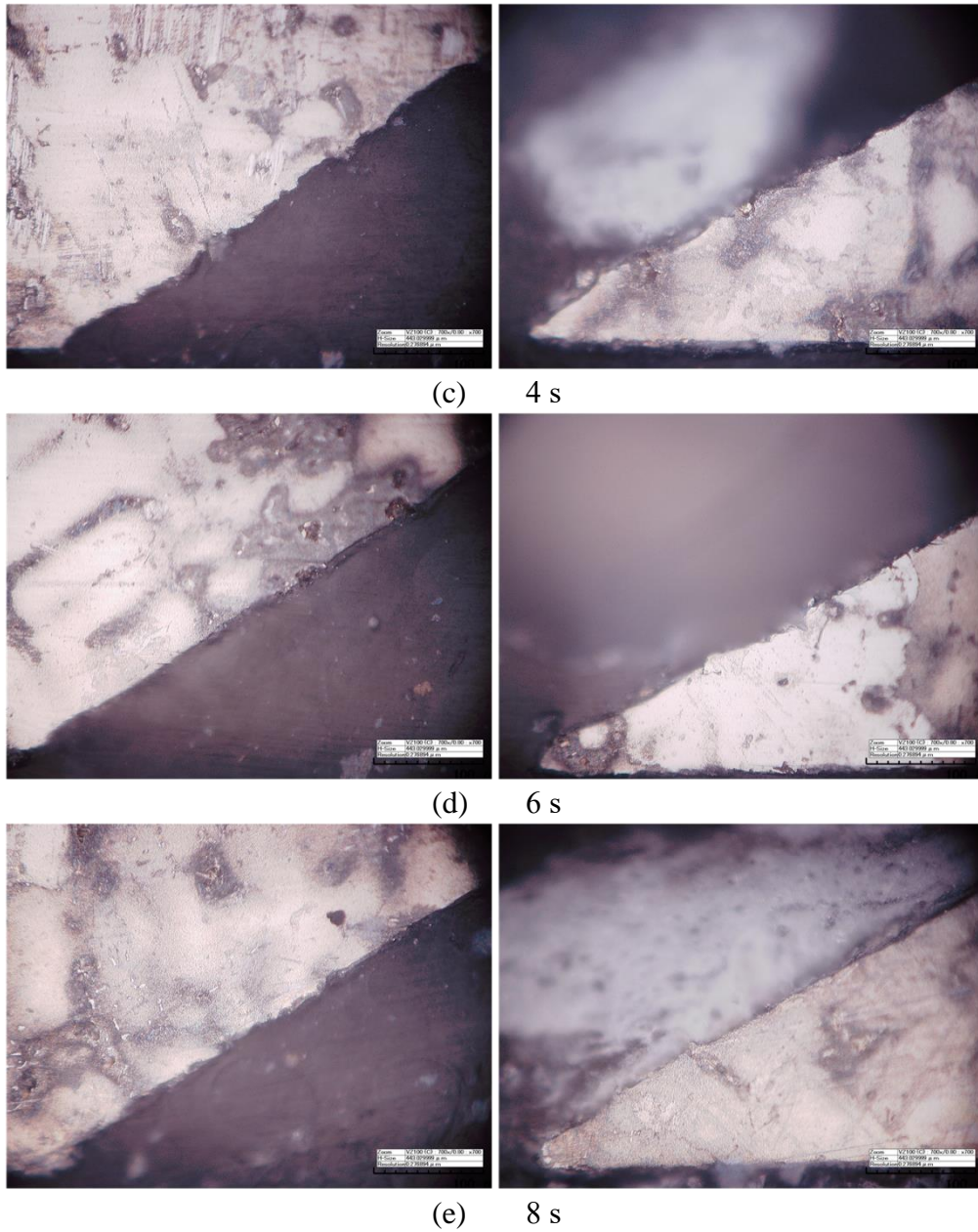


Figure 10. The residual recast layer at IMH outlets with PToE

4. CONCLUSIONS

ECDD of IMHs was used to machine the film cooling hole of turbine blades. The effect of composite processing on IMH structure was explored. The relevant processing parameters were optimized to ensure elimination of the recast layer on the IMH wall. Our study elicited three main findings.

First, with increasing PToE, the electrolytic waveform accounted for a larger proportion of the overall waveform during the pause stage of electrode. Hence, step feeding of electrode could prolong the electrolysis time.

Second, step feeding of electrode could decrease the taper, improve the wall quality, and increase the average diameter of IMHs.

Finally, once the PToE reached 4 s, the recast-layer free processing of IMHs could be realized. The longer the PToE, the more thoroughly could the recast layer be eliminated.

ACKNOWLEDGMENTS

The authors acknowledge financial support provided by the National Natural Science Foundation of China (91960204) and the Fundamental Research Funds for the Central Universities (NE2014104).

References

1. F. Klocke, A. Klink, D. Veselovac, D. K. Aspinwall, S. L. Soo, M. Schmidt, J. Schilp, G. Levy and J. P. Kruth, *CIRP Ann.-Manuf. Technol.*, 63 (2014) 703.
2. Z. Xu, Y. Wang, *Chinese J. Aeronaut.*, (2019). DOI: 10.1016/j.cja.2019.09.016.
3. Y. Yao, J. Zhou Zhang and X. Ming Tan, *Int. Commun. Heat Mass Transf.*, 52 (2014) 61.
4. P. Dai and S. X. Li, *Adv. Mater. Res.*, 971–973 (2014) 143.
5. X. Fang, N. Qu, H. Li and D. Zhu, *Int. J. Adv. Manuf. Technol.*, 68 (2013) 2005.
6. Y. Dong, X. Li, Q. Zhao, X. Li and Y. Dou, *Int. J. Adv. Manuf. Technol.*, 93 (2017) 4409.
7. J. A. McGeough, A. B. M. Khayry, W. Munro and J. R. Crookall, *CIRP Ann.-Manuf. Technol.*, 32(1983)113.
8. J. C. Hung, B. H. Yan, H. S. Liu and H. M. Chow, *J. Micromech. Microeng.*, 16(2006)1480.
9. R. Tanabe, Y. Ito, N. Mohri and T. Masuzawa, *CIRP Ann.-Manuf. Technol.*, 60 (2011) 227.
10. Y. Li, M. G. Xu, Q. H. Zhang, S. F. Ren and J. H. Zhang, *J. Mater. Process. Technol.*, 209 (2008) 1742.
11. T. Kurita and M. Hattori, *Int. J. Mach. Tools Manuf.*, 46(2006)1804.
12. D. K. Chung, H. S. Shin, B. H. Kim, M. S. Park and C. N. Chu, *J. Micromech. Microeng.*, 19(2009)1.
13. M. M. Lohrengel and C. Rosenkranz, *Corros. Sci.*, 47 (2005) 785.
14. M. D. Nguyen, M. Rahman and Y. S. Wong, *Int. J. Mach. Tools Manuf.*, 54-55(2012)55.
15. S. Plaza, J. A. Sanchez, E. Perez, R. Gil, B. Izquierdo, N. Ortega and I. Pombo, *Precis. Eng.*, 38 (2014) 821.
16. Y. Zhang, Z. Xu, D. Zhu, N. Qu, Y. Zhu, *Int. J. Adv. Manuf. Technol.*, 83 (2016) 505.
17. C. Zhang, Z. Xu, Y. Hang and J. Xing, *Int. J. Adv. Manuf. Technol.*, 103 (2019) 743.
18. M. D. Nguyen, M. Rahman and Y. S. Wong, *Int. J. Mach. Tools Manuf.*, 66 (2013) 95.
19. R. Thanigaivelan, R. M. Arunachalam and P. Drukpa, *Int. J. Adv. Manuf. Technol.*, 61(2012)1185.
20. M. P. Garg, M. Singh and S. Singh, *Micro-Machining and Process Optimization of Electrochemical Discharge Machining (ECDM) Process by GRA Method*, Springer International Publishing, (2019).
21. Y. Zhang, Z. Xu, D. Zhu and J. Xing, *Int. J. Mach. Tools Manuf.*, 92(2015)10.
22. S.K. Jui, A.B. Kamaraj, M.M. Sundaram, *J. Manuf. Process.*, 15 (2013) 460.
23. Z. W. Fan and L. W. Hourng, *Int. J. Adv. Manuf. Technol.*, 52 (2011) 555.
24. S. Ali, S. Hinduja, J. Atkinson and M. Pandya, *CIRP Ann.-Manuf. Technol.*, 58 (2009) 185.
25. Y. Zeng, L. Meng, X. Fang, *J. Electrochem. Soc.*, 164 (2017) E408.
26. Z. Q. Zeng, Y. K. Wang, Z. L. Wang, D. B. Shan and X. L. He, *Precis. Eng.*, 36 (2012) 500.
27. D.K. Chung, K.H. Lee, J. Jeong, C.N. Chu, *Int. J. Precis. Eng. Manuf.*, 15 (2014) 1785.